



Published in final edited form as:

*Genesis*. 2009 February ; 47(2): 93–106. doi:10.1002/dvg.20473.

## Aggregated P19 Mouse Embryonal Carcinoma Cells as a Simple In Vitro Model to Study the Molecular Regulations of Mesoderm Formation and Axial Elongation Morphogenesis

Yusuke Marikawa\*, Dana Ann A. Tamashiro, Toko C. Fujita, and Vernadeth B. Alarcón

Department of Anatomy, Biochemistry and Physiology, Institute for Biogenesis Research, University of Hawaii School of Medicine, Honolulu, Hawaii

### Summary

Because of their capacity to give rise to various types of cells in vitro, embryonic stem and embryonal carcinoma (EC) cells have been used as convenient models to study the mechanisms of cell differentiation in mammalian embryos. In this study, we explored the mouse P19 EC cell line as an effective tool to investigate the factors that may play essential roles in mesoderm formation and axial elongation morphogenesis. We first demonstrated that aggregated P19 cells not only exhibited gene expression patterns characteristic of mesoderm formation but also displayed elongation morphogenesis with a distinct anterior–posterior body axis as in the embryo. We then showed by RNA interference that these processes were controlled by various regulators of Wnt signaling pathways, namely  $\beta$ -catenin, Wnt3, Wnt3a, and Wnt5a, in a manner similar to normal embryo development. We further showed by inhibitor treatments that the axial elongation morphogenesis was dependent on the activity of Rho-associated kinase. Because of the convenience of these experimental manipulations, we propose that P19 cells can be used as a simple and efficient screening tool to assess the potential functions of specific molecules in mesoderm formation and axial elongation morphogenesis.

### Keywords

Wnt3; Wnt3a; Wnt5a;  $\beta$ -catenin; epiblast; convergent extension; ROCK

## INTRODUCTION

The basic body plan is conserved among all vertebrate embryos. However, the cellular and molecular mechanisms of body plan formation is less understood for mammalian embryos compared to other vertebrates, particularly with respect to germ layer specification and axis formation (Takaoka *et al.*, 2007; Tam and Loebel, 2007). The difficulty in studying the mechanisms of mammalian development is partly due to its viviparous nature: the development of the basic body plan takes place within the maternal reproductive tract. Normally, oocytes are fertilized in the oviduct and undergo a series of cell divisions to form the blastocyst, which is composed of the outer layer of trophectoderm (TE) and the internal clump of inner cell mass (ICM). TE of the blastocyst interacts with the endometrial wall of the uterus for implantation, and develops into trophoblast and extra-embryonic ectoderm. On

the other hand, ICM gives rise to the epiblast and primitive endoderm around the time of implantation. The future posterior side of the epiblast forms the primitive streak, from which cells emigrate to generate mesoderm and definitive endoderm. Mesoderm is continuously generated through the primitive streak at the posterior end of the embryo, whereas the embryonic body elongates along the anterior–posterior axis.

Because of the viviparous nature of the mammalian development, various experimental procedures, such as micromanipulations, over- and under-expression of specific gene products, and treatment with pharmacological reagents, are not easily implemented when compared with lower vertebrate embryos, like frogs and fish. In addition, maternal and extraembryonic tissues are connected to the mammalian embryo during most of development, so that the analysis of developmental mechanisms is more complicated than the lower vertebrate embryos. Mouse whole embryos can be genetically manipulated by transgenic and gene-targeting techniques, and can be cultured outside of the uterus for certain durations during experimentations (Nagy *et al.*, 2003). Nonetheless, these procedures are still laborious, time-consuming, and expensive. To compensate for these difficulties, many researchers have used *in vitro* model systems, namely cultured cell lines, which can recapitulate certain aspects of the developmental processes. For example, *in vitro* differentiation of embryonic stem (ES) cells and embryonal carcinoma (EC) cells has been used to study the mechanisms of germ layer formation because various experimental manipulations are easily implemented in these cell lines (Keller, 2005; Solter, 2006).

In the present study, we explored the mouse P19 EC cell line as an *in vitro* model to investigate the molecular mechanisms of germ layer formation and axial elongation morphogenesis. P19 cells, which were initially isolated from teratocarcinoma of normal embryo origin, possess properties similar to the epiblast, and can differentiate *in vitro* into various cell types, such as muscles and neurons (McBurney, 1993; van der Heyden and Defize, 2003). Here, we demonstrated that aggregated P19 cells exhibited gene expression patterns and axial elongation morphogenesis characteristic of posterior mesoderm, and that these processes were dependent on the same molecular components as the corresponding processes during normal development. Because various experimental manipulations can be easily and effectively applied, we propose that P19 cells can serve as a simple and convenient *in vitro* tool to assess the actions of specific molecules in mesoderm formation and axial elongation.

## RESULTS

### Aggregated P19 Cells Exhibit Gene Expression Patterns Characteristic of Posterior Mesoderm Development

Mesodermal derivatives, including cardiac and skeletal muscle, can be derived from P19 cells that are aggregated in culture medium containing 1% dimethyl sulfoxide (DMSO), indicating that mesoderm development occurs under this condition (McBurney, 1993; van der Heyden and Defize, 2003). Here, we examined by qRT-PCR the expressions of various genes during aggregation culture of P19 cells, particularly those genes that are normally expressed in the primitive streak and posterior mesoderm. P19 cells were aggregated in hanging drops of culture medium containing 1% DMSO (Fig. 1a). Each hanging drop was 20  $\mu$ L in volume, and initially contained 200 dissociated cells. After 1 day of culture (designated as Day 1), almost all cells in a drop gathered at the bottom, adhered to each other, and formed a single aggregate (Fig. 1a). Cells were harvested for RNA extraction everyday from Day 1 to Day 6 of hanging drop culture.

Many of the genes that are normally expressed in the primitive streak at E6.5 to E7.5, such as *Brachyury* (Rashbass *et al.*, 1991), *Sp5* (Harrison *et al.*, 2000), *Fgf8* (Crossley and Martin,

1995), *Snai1* (Smith et al., 1992), *Lhx1* (also known as *Lim1*; Barnes et al., 1994), *Tbx6* (Chapman et al., 1996), and *Hoxb1* (Forlani et al., 2003), were up-regulated during the first 4 days of hanging drop culture (Fig. 1b). Several members of the Wnt gene family, specifically *Wnt3* (Liu et al., 1999), *Wnt3a* (Yoshikawa et al., 1997), *Wnt5a* (Yamaguchi et al., 1999a), and *Wnt8a* (Bouillet et al., 1996), are normally expressed in the primitive streak and posterior mesoderm at E6.5 to E8.5, and they were also up-regulated in aggregated P19 cells (Fig. 1b). However, *Wnt11*, which is normally expressed in the node and extraembryonic mesoderm at E6.5 to E7.5 (Kispert et al., 1996), was not up-regulated in aggregated P19 cells. *Cdx2*, which is normally expressed in the definitive endoderm, the posterior mesoderm and the posterior neural tube at E8.5 (Beck et al., 1995), was also up-regulated during aggregation culture. By contrast, the genes that are normally associated with the maintenance of pluripotency in ES cells, such as *Pou5f1* (also known as *Oct4*; Nichols et al., 1998), *Foxd3* (Hanna et al., 2002), and *Eras* (Takahashi et al., 2003), were gradually down-regulated during aggregation culture (Fig. 1b).

The temporal order of expression of these genes during aggregation culture was also similar to that in normal development. Specifically, in aggregated P19 cells, *Wnt3* was markedly up-regulated by Day 1, followed by the upregulation of *Brachyury* by Day 2 (Fig. 1b), which is consistent with the temporal expression patterns of these genes in normal embryos (Rivera-Perez and Magnuson, 2005). *Fgf8*, *Snai1*, *Lhx1*, *Wnt3a*, *Wnt5a*, *Wnt8a*, *Tbx6*, and *Hoxb1* reached the highest expression level later than *Wnt3* and *Brachyury* (Fig. 1b), which is also similar to the temporal expression patterns during normal embryo development (Pfister et al., 2007). In addition, the up-regulation of *Hoxb5* started later than that of *Hoxb1*, and continued until Day 6 (Fig. 1b), which is consistent with the temporal expression patterns of the Hox genes in normal embryos.

### Elongation Morphogenesis of P19 Cell Aggregates

P19 cell aggregates exhibited a distinct morphological change (Fig. 1a) that is reminiscent of convergent extension of axial and paraxial mesoderm that normally takes place at the posterior end of normal embryos. Most P19 cell aggregates were nearly spherical until Day 3. However, aggregates were slightly irregular in shape at Day 4, and were clearly elongated by Day 5 and Day 6. This elongation morphogenesis was observed in almost all aggregates examined (98.5%;  $n = 199$ ), indicating that the shape change of aggregates in hanging drops occurs in a consistent and synchronous manner. Many of the aggregates (66.4%) had a single axis of elongation, whereas some aggregates had two axes (25.6%) or more than two axes (6.5%) of elongation (Fig. 1a). The elongated aggregates with a single axis exhibited a distinct morphological polarity: one end was narrower and more transparent, whereas the other end was wider and more opaque. From Day 4 to Day 6 of culture, aggregates became not only elongated in length but also constricted in width (Fig. 1a). Thus, this morphological change appears to be caused by convergent extension, which has been extensively studied in frogs and fish embryos as a unique behavior of axial and paraxial mesoderm to drive the elongation of embryo along the anterior–posterior axis (Jenny and Mlodzik, 2006; Keller et al., 1985; Wallingford et al., 2002). After Day 6, aggregates did not appear to exhibit further morphological changes, although some of them started to degenerate, as judged by the emergence of loose cells that were dissociated from the aggregates. Thus, we did not analyze aggregates beyond Day 6 in this study.

To gain insight into the relationship of aggregate elongation with respect to normal embryological events, we examined the spatial expression patterns of several genes in Day 6 aggregates by whole-mount in situ hybridization, including those that are normally expressed in the posterior mesoderm (see Fig. 2). *Brachyury*, *Cdx2*, *Wnt5a*, and *Fgf8* were strongly expressed in the narrower side of elongated aggregates. *Wnt3a* and *Tbx6* were also expressed in the narrower side of aggregates, although their expression domains were more

localized to the distal end. On the other hand, *Meox1*, which is normally expressed in the somites and anterior presomitic mesoderm but not in the posterior mesoderm at E8.5 (Conlon *et al.*, 1995), was broadly expressed in Day 6 aggregates except in the narrower end. These results suggest that the wider-narrower axis of elongated aggregates corresponds to the anterior–posterior axis of the normal embryo. *Pou5f1*, which is normally expressed only in the primordial germ cells (PGCs) at E8.5 (Scholer *et al.*, 1990), was expressed at Day 6 in a punctate manner around the middle part of aggregates (see Fig. 2). Whether these *Pou5f1*-positive cells are similar to PGCs requires further investigations.

### The Activation of Wnt/ $\beta$ -catenin Signaling Is Necessary to Up-regulate the Expression of Mesoderm Genes in P19 Cells

In normal embryos, the activation of Wnt/ $\beta$ -catenin signaling is critical for the generation of mesoderm through the primitive streak (Marikawa, 2006). Thus, we investigated whether the activation of Wnt/ $\beta$ -catenin signaling also plays a critical role in the up-regulation of mesoderm genes in P19 cell aggregates. First, we measured the level of endogenous Wnt/ $\beta$ -catenin signaling during cell aggregation, using the TOPFLASH reporter plasmid. The TOPFLASH plasmid contains a luciferase reporter gene under the transcriptional control of Lef/Tcf-response elements, and is turned on in response to active Wnt/ $\beta$ -catenin signaling (Korinek *et al.*, 1997). P19 cells were transfected with TOPFLASH, and then cultured either as a monolayer or as aggregates. The luciferase activity was higher by about 2.5- and 17.5-fold in aggregates than in a monolayer after 1 day and 2 days of culture, respectively (Fig. 3a). By contrast, the control reporter plasmid FOPFLASH, in which the Lef/Tcf-response elements are mutated, did not exhibit a significant difference between aggregate and monolayer cultures (data not shown). These results indicate that aggregation leads to the activation of endogenous Wnt/ $\beta$ -catenin signaling in P19 cells.

We then examined whether the activation of Wnt/ $\beta$ -catenin signaling is necessary for the up-regulation of mesoderm genes in P19 cell aggregates. First, P19 cells were transiently transfected with the expression plasmid encoding Dkk1, a secreted inhibitor of Wnt co-receptor Lrp5/6 (Glinka *et al.*, 1998; Mao *et al.*, 2001; Semenov *et al.*, 2001). As a control, P19 cells were transfected with the expression plasmid encoding green fluorescent protein (GFP). The expression levels of *Brachyury* and *Hoxb1* at Day 2 of hanging drop culture were lower in Dkk1-expressing aggregates than in GFP-expressing aggregates (Fig. 3b). This suggests that the inhibition of Wnt/ $\beta$ -catenin signaling impairs the up-regulation of mesoderm genes in P19 cell aggregates.

As an alternative way to inhibit Wnt/ $\beta$ -catenin signaling, we suppressed the expression of  $\beta$ -catenin in P19 cells by stably transfecting with the plasmid encoding a  $\beta$ -catenin-specific short hairpin RNA (shRNA). As a control, P19 cells were stably transfected with the plasmid encoding nontarget shRNA sequence. The stably transfected P19 cells were then aggregated in hanging drops and cultured for 2 days. In addition to its role as a mediator of Wnt/ $\beta$ -catenin signaling,  $\beta$ -catenin protein is known to regulate cadherin-mediated cell–cell adhesion (Gottardi and Gumbiner, 2001). Nonetheless, P19 cells expressing  $\beta$ -catenin-specific shRNA adhered to each other in hanging drops and formed cohesive aggregates, although their surface appeared rougher than that of control aggregates (Fig. 3c). In spite of their consistent aggregation, *Wnt3*, *Brachyury*, and *Cdx2* were not up-regulated in P19 cells expressing  $\beta$ -catenin-specific shRNA (Fig. 3d). This result further supports that the activation of Wnt/ $\beta$ -catenin signaling is essential for the up-regulation of mesoderm genes in P19 cell aggregates. Notably, the up-regulation of *Wnt3* was totally eliminated by the suppression of  $\beta$ -catenin. This suggests that the expression of *Wnt3* is regulated by the activation of Wnt/ $\beta$ -catenin signaling through a positive feedback mechanism.

In normal embryos, *Wnt3* expression in the epiblast is essential for the formation of the primitive streak (Barrow *et al.*, 2007; Liu *et al.*, 1999). Thus, we examined the role of *Wnt3* in the up-regulation of mesoderm genes in P19 cell aggregates. P19 cells were stably transfected with the plasmid encoding a *Wnt3*-specific shRNA, and then cultured as aggregates for 2 days. *Wnt3*-specific shRNA effectively reduced the expression of *Wnt3* down to about 10% of that in the control aggregates (Fig. 3e). The up-regulation of *Brachyury* and *Cdx2* was diminished in the aggregates expressing *Wnt3*-specific shRNA, when compared with those expressing the control shRNA. However, a small but distinct up-regulation of *Brachyury* and *Cdx2* was observed at Day 2. This up-regulation may be driven by *Wnt8a*, whose expression was essentially unaffected by the suppression of *Wnt3*. Nonetheless, most of the *Brachyury* and *Cdx2* expressions (more than 75% and 90%, respectively) were abolished by *Wnt3*-specific shRNA. This suggests that the up-regulation of mesoderm genes in P19 cell aggregates is mainly dependent on *Wnt3*, consistent with its role in normal embryos.

### Ectopic Activation of Wnt/ $\beta$ -catenin Signaling Is Sufficient to Up-regulate Mesoderm Genes in P19 Cells Without Cell Aggregation

We examined whether a forced activation of Wnt/ $\beta$ -catenin signaling is sufficient to up-regulate mesoderm genes in P19 cells without cell aggregation. When monolayer-cultured P19 cells were treated with *Wnt3a* protein for 1 day, many genes that are normally expressed in the primitive streak and posterior mesoderm were up-regulated, including *Brachyury*, *Wnt3*, *Wnt3a*, *Fgf8*, and *Hoxb1* (Fig. 4a). By contrast, *Foxd3* was down-regulated by the *Wnt3a* treatment (Fig. 4a). Likewise, the activation of Wnt/ $\beta$ -catenin signaling with [2',3'-E]-6-bromindirubin-3'-oxime (BIO), a specific inhibitor of GSK3 (Sato *et al.*, 2004), also induced the up-regulation of various mesoderm genes and the down-regulation of *Foxd3* in monolayer-cultured P19 cells (Fig. 4b). The expressions of *Wnt3* and *Brachyury* reached the highest levels in 24 h, whereas those of *Wnt3a*, *Hoxb1*, *Cdx2*, and *Sox17* did so only after 48 h of BIO treatment. This temporal order of mesoderm gene expression was similar to those in aggregation culture (Fig. 1b). These results suggest that the activation of Wnt/ $\beta$ -catenin signaling is sufficient to up-regulate mesoderm genes in a distinct temporal order. Notably, the expression of *Wnt3* was upregulated by the activation of Wnt/ $\beta$ -catenin signaling (Fig. 4a,b), which further supports that the expression of *Wnt3* is regulated by a positive feedback mechanism.

To compare the characteristics of P19 cells with those of the epiblast, we tested whether the activation of Wnt/ $\beta$ -catenin signaling with BIO is sufficient to up-regulate *Brachyury* in cultured embryo explants. The distal portion of E5.5 embryos were explanted and cultured for 24 h in the presence of BIO. Control explants that were cultured in the absence of BIO maintained a proamniotic cavity surrounded by the epithelial epiblast layer (Fig. 4c). None of the control explants (0 out of 17) displayed expression of *Brachyury*, as examined by *in situ* hybridization. By contrast, *Brachyury* was distinctly expressed in many of the BIO-treated explants (21 out of 24). The *Brachyury* expression was found in the inner portion (corresponding to the epiblast) but not in the outer layer (corresponding to the primitive endoderm) of the explants. These results suggest that only the epiblast, but not the primitive endoderm, possess the competence to express *Brachyury* in response to the activation of Wnt/ $\beta$ -catenin signaling. Furthermore, the proamniotic cavity was indistinct in the BIO-treated explants (Fig. 4c), suggesting that the epithelial feature of the epiblast was diminished by the activation of Wnt/ $\beta$ -catenin signaling. These results are consistent with the previous study that the constitutive activation of  $\beta$ -catenin in early embryos results in an ectopic expression of *Brachyury* and precocious epithelial-to-mesenchymal transformation of the epiblast (Kemler *et al.*, 2004). Thus, the activation of Wnt/ $\beta$ -catenin signaling is

sufficient to induce *Brachyury* expression in both the epiblast and P19 cells, demonstrating a similarity between these two types of cells.

### Wnt3a Is Essential for Mesoderm Formation and Axial Elongation in P19 Cell Aggregates

In addition to *Wnt3*, *Wnt3a* also plays a critical role in mesoderm development and axial morphogenesis in mouse embryos. In contrast to *Wnt3*, initial activation of *Brachyury* and *Tbx6* in the primitive streak is independent of *Wnt3a*, as these genes are expressed normally in *Wnt3a*-null mutant embryos at E7.5. However, *Wnt3a* is essential to maintain the expression of *Brachyury* and *Tbx6* in the posterior mesoderm, as they are markedly diminished in the mutant embryos at E8.5 (Yamaguchi *et al.*, 1999b). As a result, *Wnt3a*-null mutant embryos lack posterior somites and a tailbud at E9.5 (Takada *et al.*, 1994).

To assess the role of *Wnt3a* in mesoderm development and axial elongation in P19 cell aggregates, we suppressed the expression of *Wnt3a* by stably transfecting the plasmid encoding a *Wnt3a*-specific shRNA. Morphologically, aggregates expressing the *Wnt3a*-specific shRNA were indistinguishable from the control aggregates until Day 4 (Fig. 5a; compare with Fig. 1a). However, aggregates expressing the *Wnt3a*-specific shRNA neither elongated nor exhibited a morphological polarity by Day 6. The expression level of *Wnt3a* was effectively suppressed by shRNA, as it was reduced down to about 20% of that in the control aggregates at Day 3 (Fig. 5b). The levels of *Brachyury* were comparable at Day 2 between the aggregates expressing *Wnt3a*-specific shRNA and those expressing a control shRNA (Fig. 5b). However, the *Brachyury* level was distinctly lower in the aggregates expressing *Wnt3a*-specific shRNA after Day 2, suggesting that the maintenance of *Brachyury* expression is dependent on *Wnt3a*. Likewise, the initial up-regulation of *Cdx2* appeared unaffected until Day 3, but its expression at later stages was diminished by the suppression of *Wnt3a* (Fig. 5b). Furthermore, although the expression of early mesoderm genes, namely *Wnt3* and *Fgf8*, were not severely affected, the up-regulations of *Snai1*, *Tbx6*, and *Evx1*, which peaked at Day 3 to Day 4 in the control aggregates, were diminished by more than 50% in those expressing *Wnt3a*-specific shRNA at Day 3 (Fig. 5b). These results suggest that *Wnt3a* is essential for the up-regulation and maintenance of various mesoderm genes.

### Wnt5a Is Essential for Axial Elongation in P19 Cell Aggregates

*Wnt5a* also plays essential roles in normal axial morphogenesis in mouse embryos. *Wnt5a*-null mutant embryos exhibit a diminished caudal extension by E8.5 (Yamaguchi *et al.*, 1999a). However, *Brachyury*, *Fgf8*, and *Tbx6* are normally expressed in the caudal end of the mutant embryos, suggesting that *Wnt5a* is not essential for the initial specification of posterior mesoderm but is involved in the morphogenetic regulation of posterior mesoderm (Yamaguchi *et al.*, 1999a).

To determine whether *Wnt5a* regulates axial elongation in P19 cell aggregates, the expression of *Wnt5a* was suppressed by stably transfecting the plasmid encoding a *Wnt5a*-specific shRNA. The aggregates expressing a control shRNA as well as those expressing the *Wnt5a*-specific shRNA exhibited axial elongation by Day 6 (Fig. 6a,b). However, it appeared that axial elongation was less pronounced in the aggregates expressing *Wnt5a*-specific shRNA. This notion was confirmed by the measurement of the elongation distortion index (EDI; see Materials and Methods). The average EDI at Day 6 was significantly lower in the aggregates expressing *Wnt5a*-specific shRNA when compared with the control aggregates (Fig. 6b).

We further examined gene expressions in the aggregates expressing *Wnt5a*-specific shRNA. The expression level of *Wnt5a* was substantially reduced by shRNA down to about 10% of

that in the control aggregates at Day 3 (Fig. 6c). However, the expression of *Fgf8* was apparently unaffected by the suppression of *Wnt5a* throughout the six days of aggregation culture. Also, the up-regulation of *Brachyury* was unaffected until Day 2, although its expression was diminished by about 40% by Day 3 (Fig. 6c). These results suggest that *Wnt5a* regulates axial elongation of P19 cell aggregates without substantially affecting the initial specification of mesoderm.

Interestingly, the expression of *Pcdh8* in P19 cell aggregates was apparently unaffected by the suppression of *Wnt5a* (Figs. 1b and 6c). In *Xenopus* embryos, *Wnt5a* regulates convergent extension along the anterior–posterior body axis by activating the expression of the *Pcdh8* homolog *XPAPC*, and the depletion of *Wnt5a* by antisense morpholino oligonucleotides results in significant down-regulation of the *XPAPC* expression (Schambony and Wedlich, 2007). Thus, unlike in *Xenopus*, *Wnt5a* may not regulate axial elongation by activating the expression of *Pcdh8* in mouse embryos, although the expression pattern of *Pcdh8* in *Wnt5a*-null mutant mouse embryos is yet to be determined.

### The Activity of Rho-Associated Kinase Is Essential for Axial Elongation in P19 Cell Aggregates

Several studies have shown that *Wnt5a* protein regulates convergent extension and posterior elongation of *Xenopus* and zebrafish embryos through the Wnt/planar cell polarity (PCP) signaling pathway, which is distinct from the Wnt/ $\beta$ -catenin signaling pathway (Barrow, 2006; Karner *et al.*, 2006). Various components of the Wnt/PCP pathway have been identified that regulate convergent extension, including Rho-associated kinase (ROCK) and Jun N-terminal kinase (JNK) (Kim and Han, 2005; Marlow *et al.*, 2002; Yamanaka *et al.*, 2002). We investigated whether these PCP components are involved in the axial elongation of P19 cell aggregates. Aggregates were cultured in hanging drops of normal culture medium until Day 4, and then transferred into hanging drops containing specific inhibitors: Y27632 (ROCK inhibitor; 10  $\mu$ M), SP600125 (JNK inhibitor; 10  $\mu$ M), and U0126 (MEK inhibitor; 10  $\mu$ M). As a control, Day 4 aggregates were transferred into new hanging drops with no inhibitor. After two more days of culture (i.e., Day 6), the morphology of aggregates were assessed by measuring EDI. Neither SP600125 nor U0126 significantly inhibited the axial elongation, when compared with the control aggregates (Fig. 7a,b). SP600125 did not block axial elongation even at a near-toxic concentration (50  $\mu$ M; data not shown), which is far in excess of that typically used in cell culture. By contrast, Y27632 significantly interfered with the elongation of aggregates (Fig. 7a,b). The elongation of aggregates was also significantly inhibited by another ROCK inhibitor Fasudil (50  $\mu$ M; Fig. 7c). These results suggest that ROCK, but not JNK or MEK, is involved in the regulation of axial elongation in P19 cell aggregates.

## DISCUSSION

In the present study, we showed that aggregated P19 cells recapitulated several critical aspects of mesoderm development *in vitro*. The genes that are normally expressed in the primitive streak and posterior mesoderm were up-regulated upon cell aggregation. The initial up-regulation of mesoderm genes in P19 cell aggregates was induced by the activation of Wnt/ $\beta$ -catenin signaling, which depended on *Wnt3* and  $\beta$ -catenin, as in normal embryos. Later on, aggregates elongated by convergent extension, which is normally driven by axial and paraxial mesoderm. Elongated aggregates displayed a morphological polarity with distinct spatial gene expression patterns, which appeared to correspond to the anterior–posterior axis of the normal embryo. Elongation morphogenesis of P19 cell aggregates was dependent on the distinct actions of *Wnt3a* and *Wnt5a*, in a manner similar to the posterior development of normal embryos. Here, we propose that P19 cells can serve as a simple and

convenient in vitro tool to investigate the molecular mechanisms of mesoderm formation and axial elongation morphogenesis.

As demonstrated in this study, P19 cell aggregates can be effectively manipulated to examine the roles of specific genes in mesoderm development and axial elongation. Particularly, the knockdown of a specific gene expression can be efficiently achieved by stable transfection of a plasmid construct encoding a specific shRNA, as we have effectively down-regulated the expression of  $\beta$ -catenin, *Wnt3*, *Wnt3a*, and *Wnt5a*. Typically, by puromycin selection, it takes less than two weeks to obtain sufficient numbers of P19 cells that are stably transfected with shRNA plasmids to use for cell aggregation. Because libraries of predesigned shRNA plasmids are commercially available to target most genes in the mouse genome, P19 cells can be used as a convenient tool for the rapid screenings of candidate genes that are involved in mesoderm formation and axial elongation morphogenesis.

P19 cells can also serve as a tool to identify new genes that may be important for the initial steps of mesoderm formation. We have shown that not only cell aggregation but also ectopic activation of Wnt/ $\beta$ -catenin signaling without aggregation is sufficient to up-regulate a series of mesoderm genes that are normally expressed in the primitive streak (see Fig. 4). Microarray analyses of P19 cells that are aggregated or treated with an activator of Wnt/ $\beta$ -catenin signaling should yield a list of candidate genes that may play roles in the initial stages of mesoderm development. Furthermore, because a relatively large number of P19 cells can be easily treated with an activator of Wnt/ $\beta$ -catenin signaling, proteomics and other biochemical analyses can be implemented to identify protein modifications that may occur during mesoderm formation.

The experiment using specific inhibitors showed that the activity of ROCK between Day 4 and Day 6 is essential for the elongation of P19 cell aggregates (see Fig. 7). Elucidation of how the ROCK activity is temporally and spatially regulated during elongation morphogenesis needs further investigations, particularly with respect to the roles of Wnt/PCP pathway components, including *Wnt5a*. Our finding is consistent with the recent study that convergent extension and neural tube closure of cultured mouse embryo is diminished by the treatment with Y27632 but not with SP600125, indicating that ROCK, but not JNK, is essential for these morphogenetic processes (Ybot-Gonzales *et al.*, 2007). Thus, P19 cell aggregates can be used for simple drug treatment experiments to examine which signaling events are essential for axial elongation. Importantly, the extent of axial elongation can be quantitatively evaluated by the measurement of EDI (Fig. 7b,c).

We showed that an activator of Wnt/ $\beta$ -catenin signaling is sufficient to induce the expression of various mesoderm genes in P19 cells. In this respect, the property of P19 cells is similar to that of the epiblast in normal embryos. The activation of Wnt/ $\beta$ -catenin signaling in early embryos by a constitutive activation of  $\beta$ -catenin (Kemler *et al.*, 2004) or by a loss-of-function mutation of negative regulator Apc (Chazaud and Rossant, 2006) results in precocious and excessive expression of mesoderm genes in the epiblast. Consistently, the treatment of E5.5 distal explants with an activator of Wnt/ $\beta$ -catenin signaling caused robust expression of *Brachyury* in the epiblast, as shown in the present study. By contrast, in ES cells, the activation of Wnt/ $\beta$ -catenin signaling promotes the maintenance of the undifferentiated state (Hao *et al.*, 2006; Ogawa *et al.*, 2006; Sato *et al.*, 2004; Singla *et al.*, 2006), suggesting that the response of ES cells to active Wnt/ $\beta$ -catenin signaling is fundamentally different from those of the epiblast and P19 cells. Similarity between the epiblast and P19 cells is also exemplified by the regulatory mechanism of the *Pou5f1* gene expression. The *Pou5f1* expression in the epiblast and P19 cells are both driven by the proximal enhancer, whereas expression in ES cells is controlled by the distal



enhancer, which is also responsible for the expression in ICM and PGC (Yeom *et al.*, 1996). Although ES cells have been widely used by many researchers to study the mechanisms of mesoderm formation, the use of P19 cells should also complement the efforts to elucidate the molecular mechanisms of mesoderm formation and axial elongation.

In the past, many researchers have routinely generated mesoderm from P19 cells by aggregation culture in the presence of DMSO (van der Heyden and Defize, 2003). Nonetheless, to our knowledge, the elongation morphogenesis that we reported in the present study had not been documented. We speculate two possible reasons why such a morphogenetic event might have been overlooked. One possibility is that the duration of aggregation culture was not long enough to observe elongation morphogenesis. In many studies (e.g., Habara-Ohkubo, 1996; Ridgeway *et al.*, 2000; van der Heyden *et al.*, 2003; Vidricaire *et al.*, 1994), P19 cells were allowed to aggregate for 3 to 4 days, and then transferred to a culture dish with an adhesive substratum on which cells spread out and differentiate. By contrast, the elongation morphogenesis was most dramatic after 5 days of aggregation culture, as shown in the present study (see Fig. 1). The other possibility is that the initial cell number of each aggregate may be critical to yield elongation morphogenesis. In the present study, two hundred cells were placed in each hanging drop at the beginning of aggregation (see Fig. 1). We used this number with an intent to generate an aggregate that carries the number of cells that is similar to the epiblast of a normal embryo before primitive streak formation (Kaufman, 1995). By contrast, in several studies (e.g., Anisimov *et al.*, 2002; Smith *et al.*, 1987; Zhang *et al.*, 2002), many more cells, up to 5,000 cells, were placed in each hanging drop. Differences in aggregate size influence the type as well as the amount of mesoderm cells generated (Smith *et al.*, 1987), which may affect the pattern of morphogenetic processes.

Whether aggregates of other EC cell lines or ES cells can also exhibit the elongation morphogenesis with an anterior–posterior axis is currently unclear. F9 is one of the most commonly used EC cell lines (Lehtonen *et al.*, 1989). Although F9 cells share several features similar to ICM and ES cells, they are considered to be nullipotent and capable of differentiating only into primitive endoderm but not embryonic mesoderm (Sennerstam and Stromberg *et al.*, 1984; Zakany *et al.*, 1984). Therefore, it is unlikely that aggregates of F9 cells would exhibit convergent extension morphogenesis, which requires the activity of posterior mesoderm. By contrast, ES cells are pluripotent and capable of giving rise to any type of embryonic cells. Thus, it may be possible for ES cell aggregates to exhibit elongation morphogenesis, although it is likely to depend on a specific culture condition to effectively induce the formation of posterior mesoderm. Recently, pluripotent cell lines, called EpiSC, have been generated from the epiblast (Brons *et al.*, 2007; Tesar *et al.*, 2007). Because EpiSC cells, like P19 cells, retain various characteristics of the epiblast, it is of particular interest to examine whether EpiSC aggregates exhibit the elongation morphogenesis.

## MATERIALS AND METHODS

### Cell Culture

P19 mouse embryonal carcinoma cells were obtained from the American Type Culture Collection (Manassas, VA), and cultured in MEM Alpha Medium with 2.5% fetal bovine serum (FBS) and 7.5% calf serum (Invitrogen, Carlsbad, CA). P19 cells were aggregated by hanging drop culture (Fig. 1a). Cells were first dissociated in Trypsin-EDTA and suspended in culture medium containing 1% DMSO at 10 cells/IL density. Twenty drops of cell suspension (20  $\mu$ L each) were placed on the inner surface of the lid of a 60 mm Petri dish (351007; Becton Dickinson, Franklin Lakes, NJ). The lid with drops was carefully inverted and placed on the bottom part of a Petri dish, which was filled with about 5 mL of

phosphatebuffered saline (PBS) to minimize the evaporation of hanging drops. To activate Wnt/ $\beta$ -catenin signaling in monolayer-cultured P19 cells, the culture medium was supplemented with 100 ng/mL of recombinant mouse Wnt3a protein (R&D Systems, Minneapolis, MN) or 2  $\mu$ M [2',3'E]-6-bromoindirubin-3'-oxime (BIO; EMD Biosciences, San Diego, CA). The other pharmacological inhibitors, namely Y27632, SP600125, U0126, and Fasudil, were obtained commercially (EMD Biosciences).

### Quantitative Reverse Transcription and Polymerase Chain Reaction (qRT-PCR)

Total RNA was extracted using TRI Reagent (Molecular Research Center, Cincinnati, OH), according to the manufacturer's instruction. cDNA was synthesized from 1  $\mu$ g of total RNA, using oligo dT(18) primer and M-MLV Reverse Transcriptase (Promega, Madison, WI) in a 25  $\mu$ L reaction volume. PCR was performed using iCycler Thermal Cycler with MyiQ Single Color Real-Time PCR Detection System (Bio-Rad, Hercules, CA). 0.5  $\mu$ L of cDNA was amplified using iQ SYBR Green Supermix (Bio-Rad) in a 20  $\mu$ L reaction volume with the following condition: the initial denaturation at 94°C (5 min) followed by up to 45 cycles of 94°C (15 s), 60°C (20 s) and 72°C (40 s). The sequences of PCR primers are listed in Supporting Information. The *Gapdh* gene was used to normalize the expression levels of all other genes. At least three independent series of samples were analyzed for each experiment, and the results are presented as mean  $\pm$  standard deviation. For those experiments that are presented in Figs. 1b, 3d, 3e, 5b, and 6c, the highest gene expression level in control aggregates was set as 100% in the graphs.

### Whole-Mount in situ Hybridization

Digoxygenin-labeled antisense RNA probes were synthesized from the plasmid DNA template, using digoxigenin-11-UTP (Roche, Indianapolis, IN) and RNA polymerases (Promega). The plasmid containing the *Brachyury* cDNA was a gift from Dr. B. G. Herrmann. The cDNA fragments for *Cdx2*, *Wnt3a*, *Wnt5a*, *Tbx6*, *Fgf8*, *Meox1*, and *Pou5f1* were isolated by RT-PCR from mouse embryonic cDNA, using the primers listed in Supporting Information, and were subcloned into pGEM-T Easy vector (Promega). P19 cell aggregates and embryo explants were fixed in 4% paraformaldehyde in PBS. Probe hybridization and detection were performed according to Belo *et al.*, 1997.

### Plasmid Transfection and Luciferase Assay

A day before transfection,  $2 \times 10^4$  of P19 cells were plated per well in a 24-well plate. The plasmids were transfected using Lipofectamine2000 (Invitrogen) according to the manufacturer's instruction. The full-length cDNA of mouse *Dkk1* was obtained by RT-PCR using the primers (forward: 5'-CCA TGG TTG TGT GTG CAG CGG CAG CTG TCC GG-3' and reverse: 5'-ATT TGC GGC CGC GTG TCT CTG GCA GGT GTG GAG CCT AGA A-3'), and subcloned into the *NcoI/NotI* sites of pEF/cyto/myc (Invitrogen). The following plasmids were obtained commercially: the GFP expression plasmid (pEF/cyto/myc/GFP; Invitrogen), TOPFLASH (Upstate, Charlottesville, VA), FOPFLASH (Upstate), pRL-TK (Promega), and shRNA-encoding plasmids (TRCN 0000012692 for  $\beta$ -catenin, TRCN0000071499 for Wnt3, TRCN0000089120 for Wnt3a, TRCN0000071831 for Wnt5a, and SHC002 for nontarget control; Sigma-Aldrich, St. Louis, MO). The dual-luciferase assay was conducted using the Dual-Luciferase Reporter Assay System (Promega) with Gene Light 55 Luminometer (Microtech, Chiba, Japan), according to the manufacturer's instructions. For stable transfection, P19 cells were transfected with the shRNA-encoding plasmid that was linearized with *SfiI*, and cultured in the presence of 10  $\mu$ g/mL puromycin for at least 10 days.

## Animals and Embryo Explants

F1 (C57BL/6 × DBA/2) mice were obtained from the National Cancer Institute (Frederick, MD). Animals were maintained according to the guidelines of the Laboratory Animal Service at the University of Hawaii and the Guide for the Care and Use of Laboratory Animals of the National Research Council (Committee to Revise the Guide, Institute of Laboratory Animal Resources Council, Commission on Life Sciences, National Research Council, 1996). The protocol of animal handling and treatment was reviewed and approved by the Institutional Animal Care and Use Committee. Pregnant female mice were sacrificed at around noon of the fifth day post coitum to isolate E5.5 embryos. The distal portion of the egg cylinder was dissected using a pair of metal needles, and cultured in hanging drops of MEM Alpha Medium with 2.5% FBS and 7.5% calf serum.

## Measurement of the Elongation Distortion Index

Cell aggregates were removed from hanging drops and placed in PBS containing 5% FBS for photography. The ImageJ program (<http://rsb.info.nih.gov/ij>) was used to measure the circumference and area of individual aggregates in photographs. The elongation distortion index (EDI) was calculated as  $\{(circumference)^2/(area) \times 4\pi - 1\}$ . With this formula, when an aggregate is completely spherical, which appears circular in a photograph, the EDI is zero. The more an aggregate is elongated or distorted, the higher the EDI. EDI reflects the shape of an aggregate, and is not affected by the size of an aggregate.

## Supplementary Material

Refer to Web version on PubMed Central for supplementary material.

## Acknowledgments

We thank Dr. B. G. Herrmann for the *Brachyury* plasmid.

Contract grant sponsor: Research Center in Minority Institutions program of the National Center for Research Resources, Contract grant number: G12RR003061, Contract grant sponsor: The National Institute of Child Health and Human Development, Contract grant number: HD040208

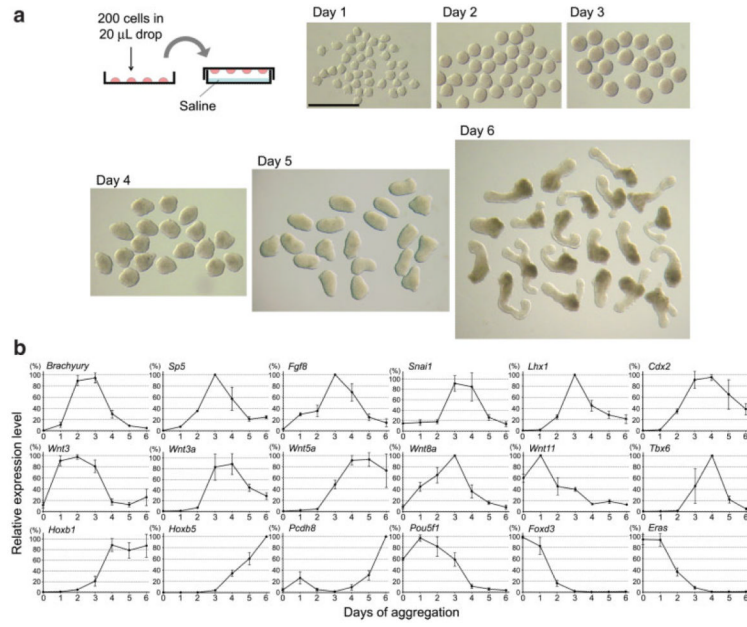
## LITERATURE CITED

- Anisimov SV, Tarasov KV, Riordon D, Wobus AM, Boheler KR. SAGE identification of differentiation responsive genes in P19 embryonic cells induced to form cardiomyocytes in vitro. *Mech Dev.* 2002; 117:25–74. [PubMed: 12204248]
- Barnes JD, Crosby JL, Jones CM, Wright CV, Hogan BL. Embryonic expression of Lim-1, the mouse homolog of *Xenopus* Xlim-1, suggests a role in lateral mesoderm differentiation and neurogenesis. *Dev Biol.* 1994; 161:168–178. [PubMed: 7904966]
- Barrow JR. Wnt/PCP signaling: A veritable polar star in establishing patterns of polarity in embryonic tissues. *Semin Cell Dev Biol.* 2006; 17:185–193. [PubMed: 16765615]
- Barrow JR, Howell WD, Rule M, Hayashi S, Thomas KR, Capecchi MR, McMahon AP. Wnt3 signaling in the epiblast is required for proper orientation of the anteroposterior axis. *Dev Biol.* 2007; 312:312–320. [PubMed: 18028899]
- Beck F, Erler T, Russell A, James R. Expression of Cdx-2 in the mouse embryo and placenta: Possible role in patterning of the extra-embryonic membranes. *Dev Dyn.* 1995; 204:219–227. [PubMed: 8573715]
- Belo JA, Bouwmeester T, Leyns L, Kertesz N, Gallo M, Follettie M, De Robertis EM. Cerberus-like is a secreted factor with neuralizing activity expressed in the anterior primitive endoderm of the mouse gastrula. *Mech Dev.* 1997; 68:45–57. [PubMed: 9431803]

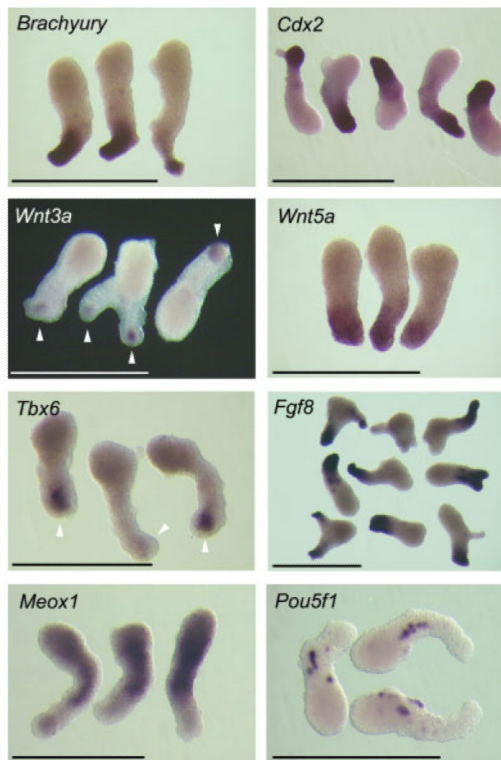
- Bouillet P, Oulad-Abdelghani M, Ward SJ, Bronner S, Chambon P, Dolle P. A new mouse member of the Wnt gene family, mWnt-8, is expressed during early embryogenesis and is ectopically induced by retinoic acid. *Mech Dev.* 1996; 58:141–152. [PubMed: 8887323]
- Brons IG, Smithers LE, Trotter MW, Rugg-Gunn P, Sun B, Chuva de Sousa Lopes SM, Howlett SK, Clarkson A, Ahrlund-Richter L, Pedersen RA, Vallier L. Derivation of pluripotent epiblast stem cells from mammalian embryos. *Nature.* 2007; 448:191–195. [PubMed: 17597762]
- Chapman DL, Agulnik I, Hancock S, Silver LM, Papaioannou VE. Tbx6, a mouse T-Box gene implicated in paraxial mesoderm formation at gastrulation. *Dev Biol.* 1996; 180:534–542. [PubMed: 8954725]
- Chazaud C, Rossant J. Disruption of early proximodistal patterning and AVE formation in *Apc* mutants. *Development.* 2006; 133:3379–3387. [PubMed: 16887818]
- Committee to Revise the Guide, Institute of Laboratory Animal Resources Council. Commission on Life Sciences, National Research Council. *Guide for the Care and Use of Laboratory Animals.* 7th edn. National Academy Press; Washington, DC: 1996.
- Conlon RA, Reaume AG, Rossant J. Notch1 is required for the coordinate segmentation of somites. *Development.* 1995; 121:1533–1545. [PubMed: 7789282]
- Crossley PH, Martin GR. The mouse *Fgf8* gene encodes a family of polypeptides and is expressed in regions that direct outgrowth and patterning in the developing embryo. *Development.* 1995; 121:439–451. [PubMed: 7768185]
- Forlani S, Lawson KA, Deschamps J. Acquisition of Hox codes during gastrulation and axial elongation in the mouse embryo. *Development.* 2003; 130:3807–3819. [PubMed: 12835396]
- Glinka A, Wu W, Delius H, Monaghan AP, Blumenstock C, Niehrs C. Dickkopf-1 is a member of a new family of secreted proteins and functions in head induction. *Nature.* 1998; 391:357–362. [PubMed: 9450748]
- Gottardi CJ, Gumbiner BM. Adhesion signaling: How beta-catenin interacts with its partners. *Curr Biol.* 2001; 11:R792–R794. [PubMed: 11591340]
- Habara-Ohkubo A. Differentiation of beating cardiac muscle cells from a derivative of P19 embryonal carcinoma cells. *Cell Struct Funct.* 1996; 21:101–110. [PubMed: 8790939]
- Hanna LA, Foreman RK, Tarasenko IA, Kessler DS, Labosky PA. Requirement for Foxd3 in maintaining pluripotent cells of the early mouse embryo. *Genes Dev.* 2002; 16:2650–2661. [PubMed: 12381664]
- Hao J, Li TG, Qi X, Zhao DF, Zhao GQ. Wnt/ $\beta$ -catenin path-way up-regulates Stat3 and converges on LIF to prevent differentiation of mouse embryonic stem cells. *Dev Biol.* 2006; 290:81–91. [PubMed: 16330017]
- Harrison SM, Houzelstein D, Dunwoodie SL, Beddington RS. Sp5, a new member of the Sp1 family, is dynamically expressed during development and genetically interacts with Brachyury. *Dev Biol.* 2000; 227:358–372. [PubMed: 11071760]
- Jenny A, Mlodzik M. Planar cell polarity signaling: A common mechanism for cellular polarization. *Mt Sinai J Med.* 2006; 73:738–750. [PubMed: 17008934]
- Karner C, Wharton KA Jr, Carroll TJ. Planar cell polarity and vertebrate organogenesis. *Semin Cell Dev Biol.* 2006; 17:194–203. [PubMed: 16839790]
- Kaufman, MH. *The atlas of mouse development* (revised edition). Academic Press; San Diego: 1995.
- Keller G. Embryonic stem cell differentiation: Emergence of a new era in biology and medicine. *Genes Dev.* 2005; 19:1129–1155. [PubMed: 15905405]
- Keller RE, Danilchik M, Gimlich R, Shih J. The function and mechanism of convergent extension during gastrulation of *Xenopus laevis*. *J Embryol Exp Morphol.* 1985; 89:185–209. [PubMed: 3831213]
- Kemler R, Hierholzer A, Kanzler B, Kuppig S, Hansen K, Taketo MM, de Vries WN, Knowles BB, Solter D. Stabilization of  $\beta$ -catenin in the mouse zygote leads to premature epithelial-mesenchymal transition in the epiblast. *Development.* 2004; 131:5817–5824. [PubMed: 15525667]
- Kim GH, Han JK. JNK and ROK $\alpha$  function in the noncanonical Wnt/RhoA signaling pathway to regulate *Xenopus* convergent extension movements. *Dev Dyn.* 2005; 232:958–968. [PubMed: 15739222]

- Kispert A, Vainio S, Shen L, Rowitch DH, McMahon AP. Proteoglycans are required for maintenance of Wnt-11 expression in the ureter tips. *Development*. 1996; 122:3627–3637. [PubMed: 8951078]
- Korinek V, Barker N, Morin PJ, van Wichen D, de Weger R, Kinzler KW, Vogelstein B, Clevers H. Constitutive transcriptional activation by a beta-catenin-Tcf complex in APC<sup>-/-</sup> colon carcinoma. *Science*. 1997; 275:1784–1787. [PubMed: 9065401]
- Lehtonen E, Laasonen A, Tienari J. Teratocarcinoma stem cells as a model for differentiation in the mouse embryo. *Int J Dev Biol*. 1989; 33:105–115. [PubMed: 2485690]
- Liu P, Wakamiya M, Shea MJ, Albrecht U, Behringer RR, Bradley A. Requirement for Wnt3 in vertebrate axis formation. *Nat Genet*. 1999; 22:361–365. [PubMed: 10431240]
- Mao B, Wu W, Li Y, Hoppe D, Stanek P, Glinka A, Niehrs C. LDL-receptor-related protein 6 is a receptor for Dickkopf proteins. *Nature*. 2001; 411:321–325. [PubMed: 11357136]
- Marikawa Y. Wnt/beta-catenin signaling and body plan formation in mouse embryos. *Semin Cell Dev Biol*. 2006; 17:175–184. [PubMed: 16765611]
- Marlow F, Topczewski J, Sepich D, Solnica-Krezel L. Zebrafish Rho kinase 2 acts downstream of Wnt11 to mediate cell polarity and effective convergence and extension movements. *Curr Biol*. 2002; 12:876–884. [PubMed: 12062050]
- McBurney MW. P19 embryonal carcinoma cells. *Int J Dev Biol*. 1993; 37:135–140. [PubMed: 8507558]
- Nagy, A.; Gertsenstein, M.; Vintersten, K.; Behringer, R. *Manipulating the mouse embryo: A laboratory manual*. 3rd edition. Cold Spring Harbor Laboratory Press; Cold Spring Harbor: 2003.
- Nichols J, Zevnik B, Anastasiadis K, Niwa H, Klewe-Nebenius D, Chambers I, Scholer H, Smith A. Formation of pluripotent stem cells in the mammalian embryo depends on the POU transcription factor Oct4. *Cell*. 1998; 95:379–391. [PubMed: 9814708]
- Ogawa K, Nishinakamura R, Iwamatsu Y, Shimamoto D, Niwa H. Synergistic action of Wnt and LIF in maintaining pluripotency of mouse ES cells. *Biochem Biophys Res Commun*. 2006; 343:159–166. [PubMed: 16530170]
- Pfister S, Steiner KA, Tam PP. Gene expression pattern and progression of embryogenesis in the immediate post-implantation period of mouse development. *Gene Expr Patterns*. 2007; 7:558–573. [PubMed: 17331809]
- Rashbass P, Cooke LA, Herrmann BG, Beddington RS. A cell autonomous function of Brachyury in T/T embryonic stem cell chimaeras. *Nature*. 1991; 353:348–351. [PubMed: 1922339]
- Ridgeway AG, Wilton S, Skerjanc IS. Myocyte enhancer factor 2C and myogenin up-regulate each other's expression and induce the development of skeletal muscle in P19 cells. *J Biol Chem*. 2000; 275:41–46. [PubMed: 10617583]
- Rivera-Perez JA, Magnuson T. Primitive streak formation in mice is preceded by localized activation of Brachyury and Wnt3. *Dev Biol*. 2005; 288:363–371. [PubMed: 16289026]
- Sato N, Meijer L, Skaltsounis L, Greengard P, Brivanlou AH. Maintenance of pluripotency in human and mouse embryonic stem cells through activation of Wnt signaling by a pharmacological GSK-3-specific inhibitor. *Nat Med*. 2004; 10:55–63. [PubMed: 14702635]
- Schambony A, Wedlich D. Wnt-5A/Ror2 regulate expression of XPAPC through an alternative noncanonical signaling pathway. *Dev Cell*. 2007; 12:779–792. [PubMed: 17488628]
- Scholer HR, Ruppert S, Suzuki N, Chowdhury K, Gruss P. New type of POU domain in germ line-specific protein Oct-4. *Nature*. 1990; 344:435–439. [PubMed: 1690859]
- Semenov MV, Tamai K, Brott BK, Kuhl M, Sokol S, He X. Head inducer Dickkopf-1 is a ligand for Wnt coreceptor LRP6. *Curr Biol*. 2001; 11:951–961. [PubMed: 11448771]
- Sennerstam R, Stromberg JO. A comparative study of the cell cycles of nullipotent and multipotent embryonal carcinoma cell lines during exponential growth. *Dev Biol*. 1984; 103:221–229. [PubMed: 6201406]
- Singla DK, Schneider DJ, LeWinter MM, Sobel BE. wnt3a but not wnt11 supports self-renewal of embryonic stem cells. *Biochem Biophys Res Commun*. 2006; 345:789–795. [PubMed: 16707109]
- Smith DE, Franco del Amo F, Gridley T. Isolation of Sna, a mouse gene homologous to the Drosophila genes snail and escargot: Its expression pattern suggests multiple roles during postimplantation development. *Development*. 1992; 116:1033–1039. [PubMed: 1295727]

- Smith SC, Reuhl KR, Craig J, McBurney MW. The role of aggregation in embryonal carcinoma cell differentiation. *J Cell Physiol.* 1987; 131:74–84. [PubMed: 2437131]
- Solter D. From teratocarcinomas to embryonic stem cells and beyond: A history of embryonic stem cell research. *Nat Rev Genet.* 2006; 7:319–327. [PubMed: 16534514]
- Takada S, Stark KL, Shea MJ, Vassileva G, McMahon JA, McMahon AP. Wnt-3a regulates somite and tailbud formation in the mouse embryo. *Genes Dev.* 1994; 8:174–189. [PubMed: 8299937]
- Takahashi K, Mitsui K, Yamanaka S. Role of ERas in promoting tumour-like properties in mouse embryonic stem cells. *Nature.* 2003; 423:541–545. [PubMed: 12774123]
- Takaoka K, Yamamoto M, Hamada H. Origin of body axes in the mouse embryo. *Curr Opin Genet Dev.* 2007; 17:344–350. [PubMed: 17646095]
- Tam PP, Loebel DA. Gene function in mouse embryogenesis: Get set for gastrulation. *Nat Rev Genet.* 2007; 8:368–381. [PubMed: 17387317]
- Tesar PJ, Chenoweth JG, Brook FA, Davies TJ, Evans EP, Mack DL, Gardner RL, McKay RD. New cell lines from mouse epiblast share defining features with human embryonic stem cells. *Nature.* 2007; 448:196–199. [PubMed: 17597760]
- van der Heyden MA, Defize LH. Twenty one years of P19 cells: What an embryonal carcinoma cell line taught us about cardiomyocyte differentiation. *Cardiovasc Res.* 2003; 58:292–302. [PubMed: 12757864]
- van der Heyden MA, van Kempen MJ, Tsuji Y, Rook MB, Jongsma HJ, Opthof T. P19 embryonal carcinoma cells: A suitable model system for cardiac electrophysiological differentiation at the molecular and functional level. *Cardiovasc Res.* 2003; 58:410–422. [PubMed: 12757875]
- Vidricaire G, Jardine K, McBurney MW. Expression of the Brachyury gene during mesoderm development in differentiating embryonal carcinoma cell cultures. *Development.* 1994; 120:115–122. [PubMed: 8119120]
- Wallingford JB, Fraser SE, Harland RM. Convergent extension: The molecular control of polarized cell movement during embryonic development. *Dev Cell.* 2002; 2:695–706. [PubMed: 12062082]
- Yamaguchi TP, Bradley A, McMahon AP, Jones S. A Wnt5a path-way underlies outgrowth of multiple structures in the vertebrate embryo. *Development.* 1999a; 126:1211–1223. [PubMed: 10021340]
- Yamaguchi TP, Takada S, Yoshikawa Y, Wu N, McMahon AP. T (Brachyury) is a direct target of Wnt3a during paraxial mesoderm specification. *Genes Dev.* 1999b; 13:3185–3190. [PubMed: 10617567]
- Yamanaka H, Moriguchi T, Masuyama N, Kusakabe M, Hanafusa H, Takada R, Takada S, Nishida E. JNK functions in the non-canonical Wnt pathway to regulate convergent extension movements in vertebrates. *EMBO Rep.* 2002; 3:69–75. [PubMed: 11751577]
- Ybot-Gonzalez P, Savery D, Gerrelli D, Signore M, Mitchell CE, Faux CH, Greene ND, Copp AJ. Convergent extension, planar-cellpolarity signalling and initiation of mouse neural tube closure. *Development.* 2007; 134:789–799. [PubMed: 17229766]
- Yeom YI, Fuhrmann G, Ovitt CE, Brehm A, Ohbo K, Gross M, Hubner K, Scholer HR. Germline regulatory element of Oct-4 specific for the totipotent cycle of embryonal cells. *Development.* 1996; 122:881–894. [PubMed: 8631266]
- Yoshikawa Y, Fujimori T, McMahon AP, Takada S. Evidence that absence of Wnt-3a signaling promotes neuralization instead of paraxial mesoderm development in the mouse. *Dev Biol.* 1997; 183:234–242. [PubMed: 9126297]
- Zakany J, Burg K, Rasko I. Spontaneous differentiation in the colonies of a nullipotent embryonal carcinoma cell line (F9). *Differentiation.* 1984; 27:146–151. [PubMed: 6479493]
- Zhang W, Yatskevych TA, Cao X, Antin PB. Regulation of Hex gene expression by a Smads-dependent signaling pathway. *J Biol Chem.* 2002; 277:45435–45441. [PubMed: 12270938]

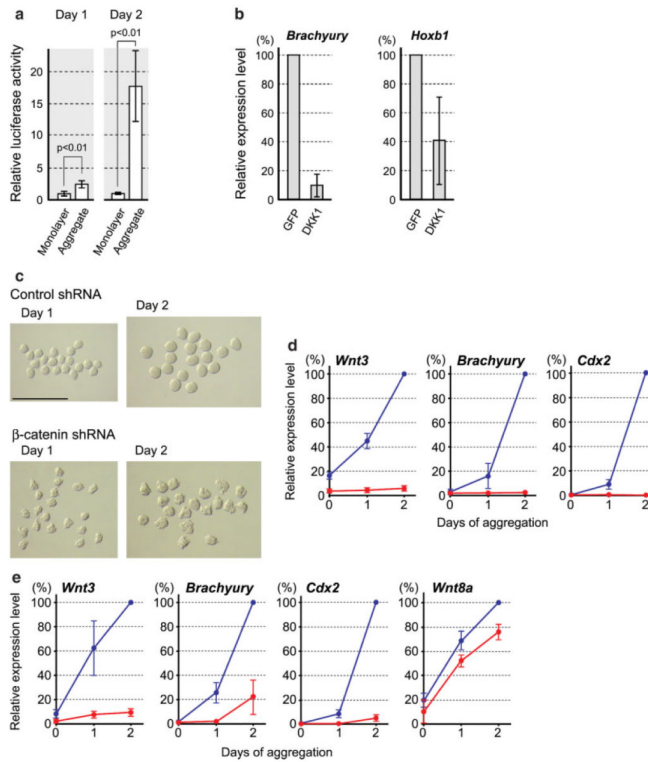


**FIG. 1.** Aggregated P19 cells exhibit distinct morphological changes and gene expression patterns. (a) A schematic diagram of hanging drop culture (top left), and morphology of aggregates from Day 1 to Day 6 of aggregation culture. Aggregates were removed from hanging drops and placed together for photography. Scale bar = 1 mm. (b) qRT-PCR analyses showing the expression levels of various genes in P19 cell aggregates from Day 0 (immediately before aggregation) to Day 6. [Color figure can be viewed in the online issue, which is available at [www.interscience.wiley.com](http://www.interscience.wiley.com).]



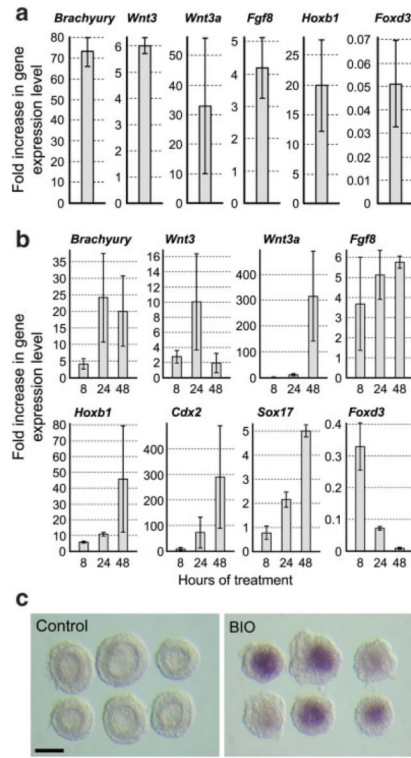
**FIG. 2.** Whole-mount in situ hybridization analyses of various genes in P19 cell aggregates at Day 6. White arrowheads indicate the locations of *Wnt3a* and *Tbx6* expression. Scale bars = 1 mm. [Color figure can be viewed in the online issue, which is available at [www.interscience.wiley.com](http://www.interscience.wiley.com).]





**FIG. 3.**

The activation of Wnt/β-catenin signaling is necessary to up-regulate the expression of mesoderm genes in P19 cells. (a) The endogenous Wnt/β-catenin signaling is elevated in response to cell aggregation. The activity of TOPFLASH is normalized by that of the cotransfected pRL-TK control plasmid. The data is presented as mean ± standard deviation of three independent experiments. Statistical significance was examined by Student's *t*-test. (b) Ectopic expression of Dkk1 impairs the up-regulation of *Brachyury* and *Hoxb1* in aggregates at Day 2. (c) Morphology of Day 1 and Day 2 aggregates that are expressing control shRNA or β-catenin-specific shRNA. Aggregates expressing β-catenin shRNA have a rougher surface. Scale bar = 1 mm. (d) The up-regulation of *Wnt3*, *Brachyury*, and *Cdx2* is essentially absent in cell aggregates expressing β-catenin-specific shRNA (red lines), as compared to those expressing the control shRNA (blue lines). (e) The up-regulation of *Brachyury* and *Cdx2* is diminished in cell aggregates expressing *Wnt3*-specific shRNA (red lines), as compared to those expressing the control shRNA (blue lines). *Wnt8a* up-regulation is unaffected by *Wnt3a* knockdown. [Color figure can be viewed in the online issue, which is available at [www.interscience.wiley.com](http://www.interscience.wiley.com).]

**FIG. 4.**

The activation of Wnt/ $\beta$ -catenin signaling is sufficient to induce the up-regulation of mesoderm genes in P19 cells without cell aggregation. Various mesoderm genes are up-regulated when monolayer-cultured P19 cells are treated with 100 ng/mL of Wnt3a protein (a) or with 2  $\mu$ M BIO (b). The vertical axes of the graphs represent fold increase of gene expressions in the treated cells relative to nontreated control cells. (c) *Brachyury* expression is activated in the distal explants of mouse E5.5 embryos by the treatment with 2  $\mu$ M BIO, as assessed by in situ hybridization. Scale bar = 100  $\mu$ m. [Color figure can be viewed in the online issue, which is available at [www.interscience.wiley.com](http://www.interscience.wiley.com).]

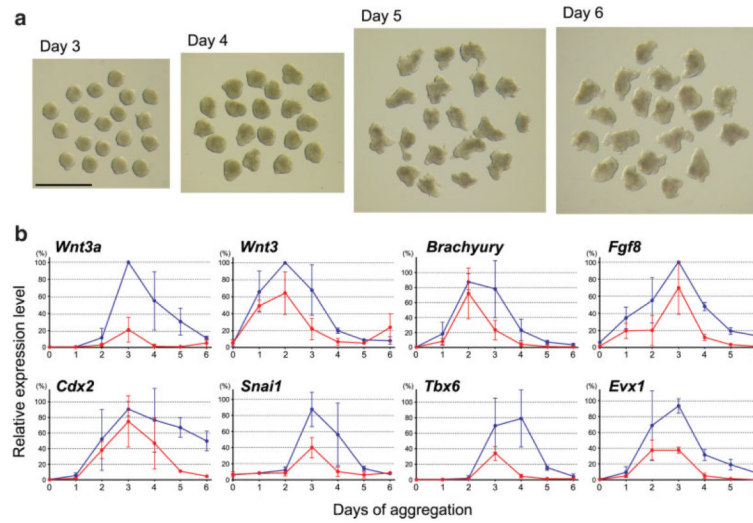


**FIG. 5.** *Wnt3a* is essential for mesoderm formation and axial elongation in P19 cell aggregates. (a) Morphology of aggregates expressing *Wnt3a*-specific shRNA. Scale bar = 1 mm. (b) Comparison of temporal gene expression patterns between aggregates expressing *Wnt3a*-specific shRNA (red lines) and those expressing the control nontarget shRNA sequence (blue lines). [Color figure can be viewed in the online issue, which is available at [www.interscience.wiley.com](http://www.interscience.wiley.com).]

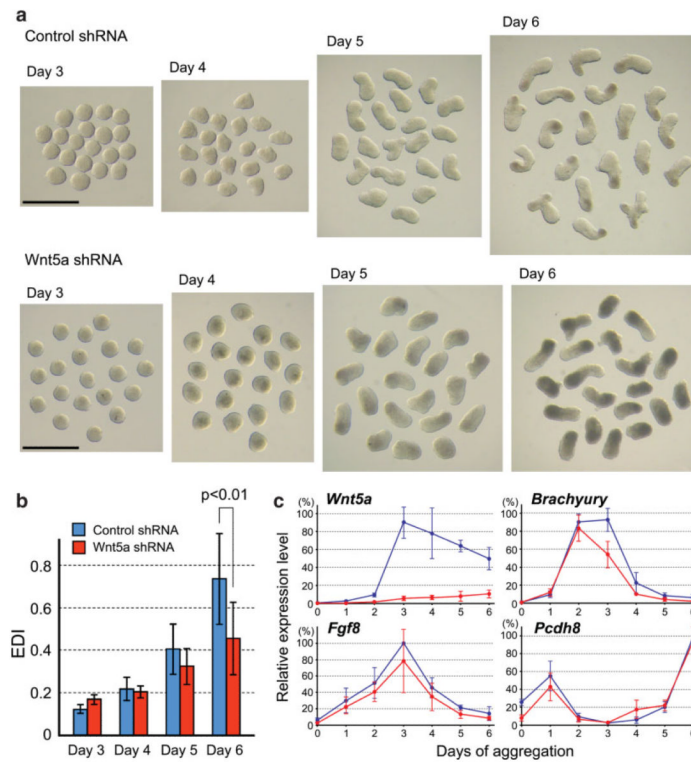


**FIG. 6.** Wnt5a is essential for axial elongation in P19 cell aggregates. (a) Morphology of aggregates expressing the control shRNA or Wnt5a-specific shRNA. Scale bar = 1 mm. (b) EDI measurement reveals that the elongation of aggregates is diminished by the suppression of Wnt5a. Statistical significance was examined by Student's *t*-test. (c) Comparison of temporal gene expression patterns between aggregates expressing Wnt5a-specific shRNA (red lines) and those expressing the control shRNA (blue lines). [Color figure can be viewed in the online issue, which is available at [www.interscience.wiley.com](http://www.interscience.wiley.com).]

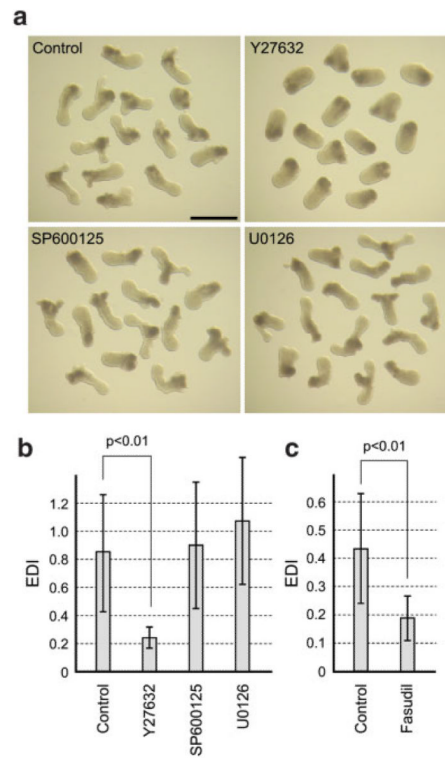


**FIG. 7.** The activity of Rho-associated kinase is essential for axial elongation in P19 cell aggregates. (a) Morphology of aggregates that are treated with a specific inhibitor from Day 4 to Day 6. Scale bar = 1 mm. (b, c) EDI measurement reveals that the elongation of aggregates is dependent on the activity of ROCK. Statistical significance was examined by Student's *t*-test. [Color figure can be viewed in the online issue, which is available at [www.interscience.wiley.com](http://www.interscience.wiley.com).]